ACS chemical biology

Letters

pubs.acs.org/acschemicalbiology

Chemoproteomic Screening of Covalent Ligands Reveals UBA5 As a Novel Pancreatic Cancer Target

Allison M. Roberts,[†] David K. Miyamoto,[†] Tucker R. Huffman,[†] Leslie A. Bateman,[†] Ashley N. Ives,[†] David Akopian,[‡] Martin J. Heslin,[§] Carlo M. Contreras,[§] Michael Rape,[‡] Christine F. Skibola,[§] and Daniel K. Nomura*[,†]

[†]Departments of Chemistry, Molecular and Cell Biology, and Nutritional Sciences and Toxicology, 127 Morgan Hall, University of California, Berkeley, Berkeley, California 94720, United States

[‡]Department of Molecular and Cell Biology, University of California, Berkeley, Berkeley, California 94720, United States

[§]The University of Alabama at Birmingham, Birmingham, Alabama 35233, United States

Supporting Information

ABSTRACT: Chemical genetic screening of small-molecule libraries has been a promising strategy for discovering unique and novel therapeutic compounds. However, identifying the targets of lead molecules that arise from these screens has remained a major bottleneck in understanding the mechanism of action of these compounds. Here, we have coupled the screening of a cysteine-reactive fragment-based covalent ligand library with an isotopic tandem orthogonal proteolysis-enabled activity-based protein profiling (isoTOP-ABPP) chemoproteomic platform to rapidly couple the discovery of lead small molecules that impair pancreatic cancer pathogenicity with the identification of druggable hotspots for potential cancer therapy. Through this coupled approach, we have discovered a covalent ligand DKM 2−93 that impairs pancreatic cancer cell survival and *in vivo* tumor growth through covalently modifying the catalytic cysteine of the ubiquitin-like modifier activating enzyme 5 (UBA5), thereby inhibiting its activity as a protein that activates the ubiquitin-like protein UFM1 to UFMylate proteins. We show that UBA5 is a novel pancreatic cancer therapeutic target and show DKM 2−93 as a relatively selective lead inhibitor of UBA5. Our results underscore the utility of coupling the screening of covalent ligand libraries with isoTOP-ABPP platforms for mining the proteome for druggable hotspots for cancer therapy.

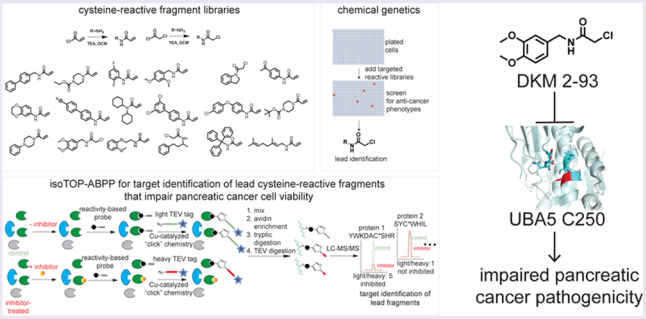

In the United States, it is estimated that over 53 000 people will be diagnosed with pancreatic cancer and over 40 000 patients will die from pancreatic cancer with a dismal overall 5-year survival rate of 7.7%.[1] Current therapeutic strategies for pancreatic cancer include resection and nonspecific therapies such as radiation or chemotherapy.[2] Unfortunately, these treatment strategies are clearly insufficient for current pancreatic cancer therapy, and better strategies are needed to discover both novel anticancer agents and targets for combatting pancreatic cancer.

Despite the identification of many novel protein targets that control cancer, a major bottleneck in this effort has been that these potential cancer therapy targets have remained largely untranslated, in part because most of these proteins are "undruggable" or difficult to target with small molecules.[3] Developing technologies that enable the coupled discovery of new cancer targets *and* small-molecule therapies would provide a promising platform to discover next-generation cures for cancer. Recently, chemoproteomic technologies have arisen to address this challenge, including activity-based protein profiling (ABPP), which uses activity or reactivity-based probes to map proteome-wide reactive, functional, and druggable hotspots directly in complex proteomes. Through competing small molecules against the binding of these chemical probes to functional and ligandable hotspots in proteins, this competitive ABPP platform provides a facile strategy for developing selective modulators against new cancer targets.[4−6] Another approach that has been successful at identifying new anticancer agents in a high throughput manner is chemical genetics, which involves small-molecule screening for anticancer phenotypes. However, a major challenge of chemical genetics is in identifying the target and mechanism of action of promising agents that arise from screens.[7,8] To address this challenge, we have coupled the screening of a fragment-based cysteine-reactive ligand library with competitive isotopic tandem orthogonal proteolysis-enabled ABPP (isoTOP-ABPP) platforms to couple the identification of covalent ligands that impair pancreatic cancer pathogenicity with the discovery of

Received: January 8, 2017
Accepted: February 10, 2017
Published: February 10, 2017

DOI: 10.1021/acschembio.7b00020
ACS Chem. Biol. XXXX, XXX, XXX−XXX

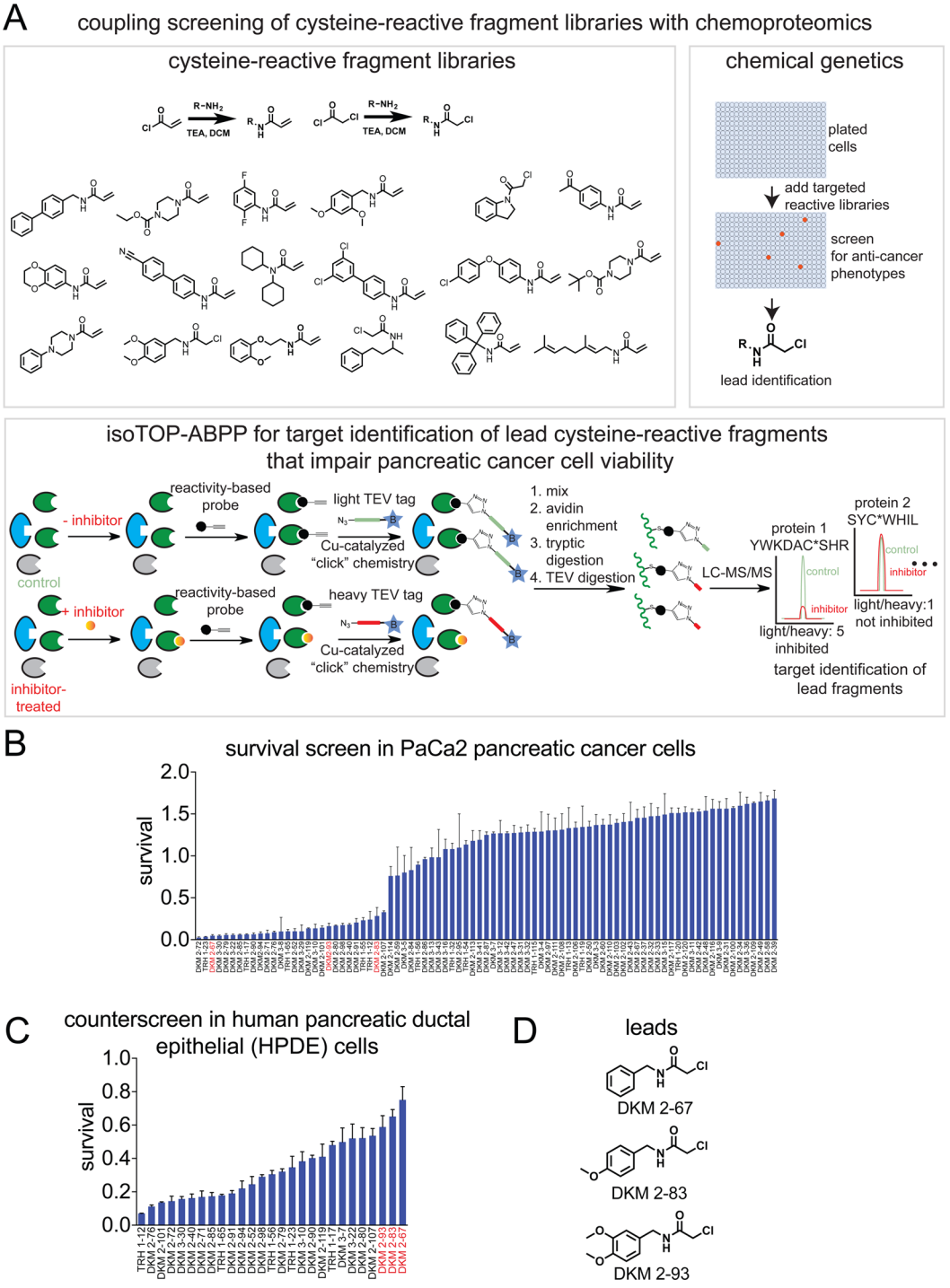

Figure 1. Coupling reactive fragment screening with isoTOP-ABPP to identify covalent ligands, targets, and druggable hotspots for pancreatic cancer. (A) We screened a library of cysteine-reactive fragments in pancreatic cancer cells to identify leads that impair pancreatic cancer pathogenicity and used isoTOP-ABPP platforms to identify the targets and site of labeling of these leads. Shown in the upper left box are examples of acrylamides and chloroacetamides that were screened here. The full composition of the library is in Table S1. (B) A library of cysteine-reactive acrylamides and chloroacetamides were screened in PaCa2 pancreatic cancer cells (50 μM) to identify any compounds that impaired PaCa2 48 h serum-free cell survival. Cell survival was assessed using Hoescht staining. (C) Leads from this screen were counterscreened in HPDE cells to identify agents that did not significantly impair serum-free cell survival in these cells. (D) Shown are lead molecules that impaired PaCa2 cell survival but showed the least degree of viability impairments in HPDE cells. Data in B and C are presented as mean ± SEM, n = 3/group. Raw data for the screen can be found in Table S2.

druggable hotspots that can be targeted for potential pancreatic cancer therapy (Figure 1A).

In this study, we screened a fragment-based covalent ligand library consisting of 85 structurally diverse cysteine-reactive acrylamide and chloroacetamides to identify compounds that impaired pancreatic cancer cell serum-free cell survival or proliferation (Figure 1B, Tables S1 and S2). Our library introduces specific covalent interactions through the incorpo-

DOI: 10.1021/acschembio.7b00020
ACS Chem. Biol. XXXX, XXX, XXX−XXX

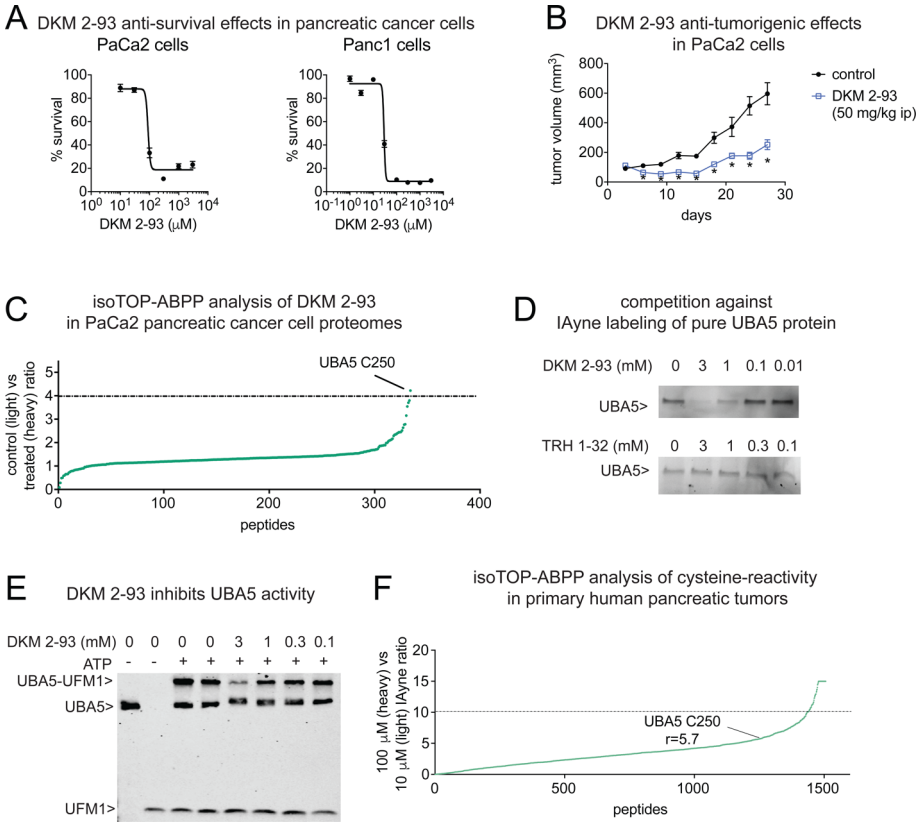

Figure 2. DKM 2−93 targets the catalytic cysteine of UBA5. (A) Dose−response of DKM 2−93 in PaCa2 and Panc1 pancreatic cancer cells in a 48 h serum-free survival assay. (B) PaCa2 tumor xenograft growth in immune-deficient SCID mice. Mice were subcutaneously injected with PaCa2 cells to initiate the tumor xenograft study, and treatments of mice were initiated with vehicle or DKM 2−93 (50 mg/kg ip, once per day) 3 days after injection of cancer cells. (C) IsoTOP-ABPP analysis of DKM 2−93 in PaCa2 cells. PaCa2 proteomes were pretreated with DMSO or DKM 2−93 (50 μM) prior to labeling proteomes with IAyne and appending a biotin-azide handle bearing a TEV protease recognition site and an isotopically light (for DMSO-treated) and heavy (for DKM 2−93-treated) tag. DMSO and DKM 2−93-treated proteomes were then mixed in a 1:1 ratio and subsequently avidin-enriched, tryptically digested, and then probe-modified tryptic peptides were released by TEV protease and analyzed using quantitative proteomic approaches. Peptide ratios shown are average ratios for those probe-modified peptides that were identified in at least two out of three biological replicates. A light to heavy ratio of 1 indicates that the probe-labeled cysteine-bearing peptide was not bound by DKM 2−93, whereas a ratio >3 indicates bound sites. (D) Gel-based ABPP validation of UBA5 as a target of DKM 2−93. DMSO or DKM 2−93 was preincubated with pure human UBA5 (30 min) prior to labeling with IAyne (10 μM, 30 min), followed by rhodamine-azide conjugation by CuAAC, SDS/PAGE, and readout of gel fluorescence. Shown is a representative gel from n = 3. (E) UBA5 activity assay. UBA5 was preincubated with DMSO or DKM 2−93, then UFM1 and ATP were added to initiate the reaction. DTT is used as a negative control to release the UBA5-UFM1 thioester linkage. Shown is a representative gel from n = 3. (F) IsoTOP-ABPP analysis of cysteine-reactivity in pooled primary human pancreatic ductal adenocarcinoma tumors. Ten primary human pancreatic tumor lysates were pooled together and labeled with 100 or 10 μM of IAyne followed by subsequent isoTOP-ABPP analysis. Shown are ratios of heavy (100 μM) to light (10 μM) peptides. Data in A and B are presented as mean ± SEM, n = 5−8/group. Significance is expressed as $^*p < 0.05$ compared to vehicle-treated or siControl or shControl cells. Raw and processed isoTOP-ABPP data for C and F can be found in Table S3.

ration of cysteine-reactive acrylamide and chloroacetamide warheads (Table S1). Recent studies by Backus *et al.* have shown that the reactivity of these cysteine-reactive covalent ligands can be made to confer substantial selectivity against specific ligandable hotspots in complex proteomes.[6] These small molecular weight fragment-based covalent ligands enable sampling of more macromolecular protein space and druggable hotspots.[9] Most importantly, this approach can also be coupled with isoTOP-ABPP platforms for rapid target discovery through the competition of covalent ligand hits against reactivity-based probes without the need for additional derivatization of the compounds.

Through this screening effort, we identified 27 hits that impaired PaCa2 pancreatic cancer cell survival or proliferation by greater than 70% (Figure 1B; Table S2). To rule out compounds that may nonspecifically cause toxicity, we also counterscreened these hits against immortal human pancreatic ductal epithelial (HPDE) cells to eliminate compounds that impaired survival or proliferation by >50% in HPDE cells (Figure 1C, Table S2). Through this screening effort, we identified three main chloroacetamide hits DKM 2−67, DKM 2−83, and DKM 2−93 (Figure 1D). We chose to pursue DKM 2−93 for target identification using isoTOP-ABPP approaches.

We show that DKM 2−93 not only impairs pancreatic cancer cell survival in PaCa2, but also Panc1 cells with 50% effective concentration values of 90 and 30 μM, respectively (Figure 2A). Surprisingly, even though the structure of DKM 2−93 is quite simple, we show that DKM 2−93 daily treatment significantly impairs tumor growth of PaCa2 cells *in vivo* in tumor xenograft studies in immune-deficient mice without causing any weight loss or overt toxicity (Figure 2B; Figure S1).

Next, we used competitive isoTOP-ABPP platforms to identify the specific druggable hotspot targeted by DKM 2−93 to impair pancreatic cancer pathogenicity (Figure 2C; Table

DOI: 10.1021/acschembio.7b00020
ACS Chem. Biol. XXXX, XXX, XXX−XXX

S3). We competed DKM 2−93 directly against labeling of PaCa2 pancreatic cancer cell proteomes with the broad cysteine-reactive iodoacetamide-alkyne (IAyne) probe for subsequent isoTOP-ABPP quantitative proteomic analysis. We then only interpreted ratios from probe-modified peptides that showed up across at least two out of three biological replicates. This resulted in the analysis of 335 probe-modified peptides of which most of these peptides (313 peptides) showed ratios less than 2, showing that DKM 2−93 did not nonspecifically react with large numbers of protein targets. Among these probe-modified peptides, only one target showed a light to heavy probe-modified peptide ratio >4. This top hit was cysteine 250 (C250) on ubiquitin-like modifier activating enzyme 5 (UBA5), showing an isotopic ratio of 4.2 (Figure 2C; Table S3). C250 is the catalytic cysteine on UBA5, suggesting that DKM 2−93 is a direct inhibitor of UBA5.[10,11] UBA5 is a protein involved in activating a ubiquitin-like protein UFM1 to UFMylate proteins.[10,12] While UBA5 and UFMylation have been shown to be important in breast cancer through UFM1 conjugation of a nuclear receptor coactivator ASC1 that modulates estrogen receptor signaling,[13] UBA5 has not been previously attributed to pancreatic cancer pathogenicity, thus making it a potentially novel pancreatic cancer therapeutic target. We show validation of UBA5 as a target of DKM 2−93 through competition of DKM 2−93 against IAyne labeling of pure human UBA5 using gel-based ABPP methods (Figure 2D). To further show that this interaction is relatively specific, we demonstrate that another cysteine-reactive fragment that did not impair PaCa2 survival, TRH 1−32, does not inhibit IAyne labeling of UBA5 (Figure 2D). Consistent with our data showing that DKM 2−93 binds to the catalytic cysteine of UBA5, we also show that UBA5 activity, represented by activation and conjugation of UFM1 on C250 on UBA5 (UFM1-UBA5 complex), is inhibited by DKM 2−93 with an 50% inhibitory concentration of 430 μM (Figure 2E). This value is within 5-fold of the EC50 value of this compound in PaCa2 cells.

We also performed isoTOP-ABPP profiling to quantitatively map proteome-wide cysteine reactivity in pooled primary human pancreatic tumors to determine whether UBA5 exists in pancreatic cancer and also to ascertain the relative reactivity of UBA5 C250 within the proteome. To map the relative reactivity of each cysteine in primary pancreatic tumors, we labeled pooled pancreatic tumor proteomes with either a high (100 μM, heavy) or low (10 μM, light) concentration of IAyne and assessed the quantitative heavy to light ratios of probe-labeled peptides. Previous studies mapping cysteine reactivity in this manner have shown that a ratio of <3 would indicate a hyper-reactive and likely functional cysteine, whereas a ratio ∼10 would not be considered particularly reactive.[14] We indeed showed that UBA5 protein is present in primary human pancreatic tumors and that C250 of UBA5 shows a heavy (100 μM) to light (10 μM) ratio of 4.7, indicating that this cysteine is just moderately hyper-reactive, despite C250 representing the catalytic cysteine of this enzyme (Figure 2F). This lack of hyper-reactivity may be possibly due to the exquisite substrate specificity of UBA5 for a large protein substrate such as UFM1, where the reactivity of C250 on UBA5 may be tempered to prevent promiscuous substrate recognition. Nonetheless, we show that UBA5 is present in primary human pancreatic tumors and that the catalytic C250 is accessible in these tumors.

To further confirm that UBA5 inactivation impairs pancreatic cancer pathogenicity, we also knocked down the expression of UBA5 in Paca2 cells (Figure 3A). We show that short interfering RNA (siRNA)-mediated transient or short hairpin RNA (shRNA)-mediated stable genetic knockdown of UBA5 in PaCa2 cells phenocopies DKM 2−93 in impairing Paca2 serum-free cell survival and *in vivo* tumor xenograft growth (Figure 3B,C).

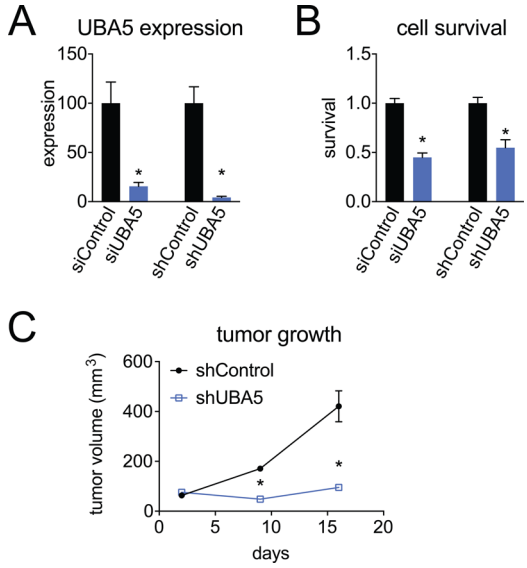

Figure 3. Impairment of pancreatic cancer pathogenicity by UBA5 knockdown. (A) UBA5 expression in Paca2 cells. UBA5 was transiently knocked down with siRNA and stably knocked down with shRNA, and expression was determined by qPCR. (B) Serum-free cell survival (48 h) from transient siRNA or stable shRNA knockdown of UBA5 in PaCa2 cells. (C) Tumor xenograft growth of shControl and shUBA5 Paca2 cells in immune-deficient SCID mice. Data are presented as mean ± SEM, n = 3−6/group. Significance is expressed as $^*p < 0.05$ compared to siControl or shControl cells.

Here, we have coupled chemical genetic screening of a covalent ligand library with isoTOP-ABPP platforms to discover a cysteine-reactive fragment DKM 2−93 that inhibits UBA5 to impair pancreatic cancer pathogenicity. A previous study has reported an organometallic UBA5 inhibitor that acts through noncompetitive mechanisms;[15] DKM 2−93 represents another potential inhibitor scaffold that acts through covalent modification of the catalytic cysteine that can potentially be used to generate more potent and selective UBA5 inhibitors. It will be of future interest to determine the UFMylation protein substrates of UBA5 that are responsible for the effects observed here, toward better understanding the mechanism through which UBA5 controls pancreatic cancer pathogenicity. We also cannot rule out other potential targets of DKM 2−93 which may contribute to its anticancer activity. While C250 of UBA5 was the only target of DKM 2−93 showing a light to heavy peptide ratio of >4, there were four additional targets that showed ratios >3—UQCRC1, SLC25A3, a TAP2, and CATSPERD—which may also play roles in DKM 2−93 action. Furthermore, DKM 2−93 may act with additional targets outside of those profiled by the iodoacetamide-alkyne cysteine reactive probe used in this study. Thus, it may be of future interest to develop a biorthogonal probe based on the DKM 2−93 structure.

Taken more broadly, our results underscore the utility of combining covalent ligand screening with chemoproteomic

DOI: 10.1021/acschembio.7b00020
ACS Chem. Biol. XXXX, XXX, XXX−XXX

platforms to rapidly mine the proteome for druggable hotspots that can be exploited for potential cancer therapy.

METHODS

Materials. IAyne was obtained from CHESS Gmbh. HIS_6–UBA5 and HIS_6–UFM1 were purchased from Boston Biochem. shRNA constructs were obtained from Sigma-Aldrich. Primers were obtained from Elim Pharmaceuticals. The composition of the cysteine-reactive library is in Table S1. The synthesis and characterization of most this library will be reported in a subsequent manuscript. The description of part of the cysteine-reactive library of covalent ligands is described in the Supporting Information.

Cell Culture. Mia-PaCa2 and Panc1 cells were purchased from ATCC and were grown in DMEM with 10% FBS. HPDE cells were obtained from Rushika Perera's laboratory at UCSF and grown in Life Technologies Keratinocyte SFM combo (cat no: 17005042). The generation of these cells have been previously described.[16]

Survival and Proliferation Assays. Cells were plated the evening before the experiment and allowed to adhere overnight. For both survival and proliferation assays, cells were plated in regular media. Before dosing, the medium was aspirated from all wells and replaced with the appropriate medium and drug dosage. For the chemical genetics screen, cells were treated with either DMSO or the cysteine-reactive fragment for 48 h, and cell viability was assessed by Hoescht stain using our previously described methods.[17]

Tumor Xenografts. C.B17 SCID male mice (6–8 weeks old) were injected subcutaneously into the flank with 2 000 000 cells as previously described.[17] After 3 days, the mice were exposed by intraperitoneal (ip) injection with either vehicle (18:1:1 PBS/ethanol/PEG40) or 50 mg/kg DKM-293 once per day, each day for the duration of the study. Tumors were measured every 3 days by caliper measurements. Animal experiments were conducted in accordance with the guidelines of the Institutional Animal Care and Use Committee of the University of California, Berkeley.

Proteomic Analysis. IsoTOP-ABPP analyses were performed as previously described.[6,14] PaCa2 cell lysates were preincubated with DMSO vehicle or DKM 2–93 (50 μM) for 30 min at 37 °C and then labeled with IAyne (100 μM) for 1 h at RT. They were subsequently treated with isotopically light (control) or heavy (treated) TEV-biotin 100 μM, and click chemistry was performed as previously described.[6,14] Proteins were precipitated and pelleted by centrifugation. Proteins were washed 3 times with cold methano,l then denatured and resolubilized by heating in 1.2% SDS/PBS to 85 °C for 5 min. Insoluble components were precipitated by centrifugation at 6500*g*, and soluble proteome was diluted in 5 mL of PBS, for a final concentration of 0.2% SDS. Labeled proteins were bound to avidin-agarose beads (170 μL beads from Thermo Pierce) while rotating overnight at 4 °C. Bead-linked proteins were then washed three times each in PBS and water, resuspended in 6 M urea/PBS, and reduced in dithiothreitol (1 mM), alkylated with iodoacetamide (18 mM), then washed and resuspended in 2 M urea/PBS with 1 mM calcium chloride and trypsinized overnight (0.5 μg/μL sequencing grade trypsin from Promega). Tryptic peptides were discarded, and beads were washed three times each in PBS and water, then washed with TEV buffer containing DTT (1 μM). TEV-biotin tag was digested overnight in TEV buffer containing DTT (1 μM) and Ac-TEV protease (5 μL) at 29 °C. Peptides were diluted in water and acidified with final concentration of 5% formic acid.

Peptides from all proteomic experiments were pressure-loaded onto a 250 μm inner diameter fused silica capillary tubing packed with 4 cm of Aqua C18 reverse-phase resin (Phenomenex # 04A-4299), which was previously equilibrated. The peptides loaded onto this capillary tubing were then attached using a MicroTee PEEK 360 μm fitting (Thermo Fisher Scientific #p-888) to a 13 cm laser pulled column packed with 10 cm Aqua C18 reverse-phase resin and 3 cm of strong-cation exchange resin for isoTOP-ABPP studies. Samples were analyzed using a Q Exactive Plus mass spectrometer (Thermo Fisher Scientific) using a Multidimensional Protein Identification Technology (MudPIT) program as previously described.[6,14] Data were collected in data-dependent acquisition mode with dynamic exclusion enabled (60 s). One full MS (MS1) scan (400–1800 m/z) was followed by 15 MS2 scans of the most abundant ions. Heated capillary temperature was set to 200 °C, and the nanospray voltage was set to 2.75 kV.

For MudPIT runs, samples were run with the following five-step MudPIT program (using 0%, 10%, 25%, 80%, and 100% salt bumps). Data were extracted in the form of MS1 and MS2 files using Raw Extractor 1.9.9.2 (Scripps Research Institute) and searched against the Uniprot mouse database using the ProLuCID search methodology in IP2 v.3 (Integrated Proteomics Applications, Inc.).[18] Cysteine residues were searched with a static modification for carboxyaminomethylation (+57.02146) and up to two differential modifications for either the light or heavy TEV tags (+464.28596 or +470.29977, respectively). Peptides were required to have at least one tryptic end and to contain the TEV modification. ProLUCID data were filtered through DTASelect to achieve a peptide false-positive rate below 1%.

Gel-Based ABPP. Gel-based ABPP methods were performed as previously described.[19] HIS_6–UBA5 (0.06 μg) protein was pretreated with DMSO or DKM 2–93 for 30 min at RT in an incubation volume of 50 μL of PBS and were subsequently treated with IAyne (10 μM final concentration) for 30 min at 37 °C. Copper-catalyzed azide–alkyne cycloaddition "click chemistry" was performed to append rhodamine-azide onto IAyne probe-labeled proteins. The samples were separated by SDS/PAGE and scanned using a ChemiDoc MP (Bio-Rad Laboratories, Inc.). Inhibition of target labeling was assessed by densitometry using ImageStudio Light software.

UBA5 Activity Assay. HIS_6–UBA5 and HIS_6–UFM1 were purchased from Boston Biochem. UBA5 (1.25 μM) was preincubated for 30 min with either DMSO or DKM 2–93 in buffer (50 mM Tris-HCl, pH 7, 5 mM $MgCl_2$), and then incubated with UFM1 (52.5 μM) ATP (1 μM) for 90 min at RT, after which the reaction was quenched in 6× nonreducing loading dye, and proteins were separated on a 4–20% TGX nonreducing denaturing gel, followed by Western blot analysis using anti-HIS_6 antibody (Abcam, ab18184).

UBA5 Knockdown. UBA5 was knocked down transiently with siRNA or stably with shRNA as previously described.[17,20] For siRNA studies, PaCa2 cells (200 000 cells/well) were seeded overnight, after which siControl (nontargeting siRNA) or siUBA5 siRNA oligonucleotides (five pooled siRNAs targeting UBA5 purchased from Dharmacon) were transfected into cells using Dharmafect 2. Cells were harvested after 48 h for qPCR and for seeding for cell viability assays.

For shRNA studies, shControl (targeting GFP) and shUBA5 constructs (purchased from Sigma) were transfected into HEK293T cells alongside lentiviral vectors using Lipofectamine 2000. Lentivirus was collected from filtered cultured medium 48 h post-transfection and used to infect the target cancer cell line with Polybrene (0.01 mg mL^{-1}). Target cells were selected over 3 days with 1 mg mL^{-1} puromycin. The short-hairpin sequence used for generation of the UBA5 knockdown lines was CCGGCCTCAGTGTGATGACA-GAAATCTCGAGATTTCTGTCATCACACTGAGGTTTT. The control shRNA was targeted against GFP with the target sequence GCAAGCTGACCCTGAAGTTCAT. Knockdown was confirmed by qPCR.

qPCR. qPCR was performed using the manufacturer's protocol for Fisher Maxima SYBR Green with 10 mM primer concentrations or for Bio-Rad SsoAdvanced Universal Probes Supermix. Primer sequences for Fisher Maxima SYBR Green were derived from Primer Bank. Primer sequences for Bio-Rad SsoAdvanced Universal Probes Supermix were designed with Primer 3 Plus.

Primary Human Pancreatic Tumors. Eligible patients completed written consent for our tissue banking protocol that is approved by the University of Alabama at Birmingham Institutional Review Board. During the pancreatic tumor resection, a 1 cm^3 portion of the tumor was dissected free of the fresh resection specimen, divided into 4–5 aliquots, placed into 1.5 mL cryovials, flash frozen, and stored at −80 °C. Adjacent nontumor bearing pancreatic tissue was also collected and banked in a similar manner.

DOI: 10.1021/acschembio.7b00020
ACS Chem. Biol. XXXX, XXX, XXX–XXX

■ ASSOCIATED CONTENT

Supporting Information

The Supporting Information is available free of charge on the ACS Publications website at DOI: 10.1021/acschembio.7b00020.

Additional methods; Figure S1; and Table legends for Tables S1, S2, and S3 (PDF)
Table S1 (XLSX)
Table S2 (XLSX)
Table S3 (XLSX)

■ AUTHOR INFORMATION

Corresponding Author

*E-mail: dnomura@berkeley.edu.

ORCID

Daniel K. Nomura: 0000-0003-1614-8360

Notes

The authors declare no competing financial interest.

■ ACKNOWLEDGMENTS

We thank the members of the Nomura Research Group for critical reading of the manuscript. This work was supported by grants from the National Institutes of Health (R01CA172667 for D.K.N., A.M.R., T.R.H., D.K.M., and L.A.B. and Chemical Biology Training Grant T32 GM066698 for A.M.R.), American Cancer Society Research Scholar Award (RSG14-242-01-TBE for D.K.N., A.M.R., D.K.M., L.A.B.), and the UAB/UMN SPORE in Pancreatic Cancer, Clinical Core (NIH P50 CA101955).

■ REFERENCES

(1) NIH-SEER database.
(2) Garrido-Laguna, I., and Hidalgo, M. (2015) Pancreatic cancer: from state-of-the-art treatments to promising novel therapies. *Nat. Rev. Clin. Oncol. 12*, 319−334.
(3) Dixon, S. J., and Stockwell, B. R. (2009) Identifying druggable disease-modifying gene products. *Curr. Opin. Chem. Biol. 13*, 549−555.
(4) Nomura, D. K., Dix, M. M., and Cravatt, B. F. (2010) Activity-based protein profiling for biochemical pathway discovery in cancer. *Nat. Rev. Cancer 10*, 630−638.
(5) Roberts, A. M., Ward, C. C., and Nomura, D. K. (2016) Activity-based protein profiling for mapping and pharmacologically interrogating proteome-wide ligandable hotspots. *Curr. Opin. Biotechnol. 43*, 25−33.
(6) Backus, K. M., Correia, B. E., Lum, K. M., Forli, S., Horning, B. D., González-Páez, G. E., Chatterjee, S., Lanning, B. R., Teijaro, J. R., Olson, A. J., Wolan, D. W., and Cravatt, B. F. (2016) Proteome-wide covalent ligand discovery in native biological systems. *Nature 534*, 570−574.
(7) Gangadhar, N. M., and Stockwell, B. R. (2007) Chemical genetic approaches to probing cell death. *Curr. Opin. Chem. Biol. 11*, 83−87.
(8) Smukste, I., and Stockwell, B. R. (2005) Advances in chemical genetics. *Annu. Rev. Genomics Hum. Genet. 6*, 261−286.
(9) Edfeldt, F. N. B., Folmer, R. H. A., and Breeze, A. L. (2011) Fragment screening to predict druggability (ligandability) and lead discovery success. *Drug Discovery Today 16*, 284−287.
(10) Gavin, J. M., Hoar, K., Xu, Q., Ma, J., Lin, Y., Chen, J., Chen, W., Bruzzese, F. J., Harrison, S., Mallender, W. D., Bump, N. J., Sintchak, M. D., Bence, N. F., Li, P., Dick, L. R., Gould, A. E., and Chen, J. J. (2014) Mechanistic study of Uba5 enzyme and the Ufm1 conjugation pathway. *J. Biol. Chem. 289*, 22648−22658.
(11) Bacik, J.-P., Walker, J. R., Ali, M., Schimmer, A. D., and Dhe-Paganon, S. (2010) Crystal Structure of the Human Ubiquitin-activating Enzyme 5 (UBA5) Bound to ATP MECHANISTIC INSIGHTS INTO A MINIMALISTIC E1 ENZYME. *J. Biol. Chem. 285*, 20273−20280.
(12) Wei, Y., and Xu, X. (2016) UFMylation: A Unique & Fashionable Modification for Life. *Genomics, Proteomics Bioinf. 14*, 140−146.
(13) Yoo, H. M., Kang, S. H., Kim, J. Y., Lee, J. E., Seong, M. W., Lee, S. W., Ka, S. H., Sou, Y.-S., Komatsu, M., Tanaka, K., Lee, S. T., Noh, D. Y., Baek, S. H., Jeon, Y. J., and Chung, C. H. (2014) Modification of ASC1 by UFM1 is crucial for ERα transactivation and breast cancer development. *Mol. Cell 56*, 261−274.
(14) Weerapana, E., Wang, C., Simon, G. M., Richter, F., Khare, S., Dillon, M. B. D., Bachovchin, D. A., Mowen, K., Baker, D., and Cravatt, B. F. (2010) Quantitative reactivity profiling predicts functional cysteines in proteomes. *Nature 468*, 790−795.
(15) da Silva, S. R., Paiva, S.-L., Bancerz, M., Geletu, M., Lewis, A. M., Chen, J., Cai, Y., Lukkarila, J. L., Li, H., and Gunning, P. T. (2016) A selective inhibitor of the UFM1-activating enzyme, UBA5. *Bioorg. Med. Chem. Lett. 26*, 4542−4547.
(16) Perera, R. M., Stoykova, S., Nicolay, B. N., Ross, K. N., Fitamant, J., Boukhali, M., Lengrand, J., Deshpande, V., Selig, M. K., Ferrone, C. R., Settleman, J., Stephanopoulos, G., Dyson, N. J., Zoncu, R., Ramaswamy, S., Haas, W., and Bardeesy, N. (2015) Transcriptional control of autophagy-lysosome function drives pancreatic cancer metabolism. *Nature 524*, 361−365.
(17) Louie, S. M., Grossman, E. A., Crawford, L. A., Ding, L., Camarda, R., Huffman, T. R., Miyamoto, D. K., Goga, A., Weerapana, E., and Nomura, D. K. (2016) GSTP1 Is a Driver of Triple-Negative Breast Cancer Cell Metabolism and Pathogenicity. *Cell Chem. Biol. 23*, 567−578.
(18) Xu, T., Park, S. K., Venable, J. D., Wohlschlegel, J. A., Diedrich, J. K., Cociorva, D., Lu, B., Liao, L., Hewel, J., Han, X., Wong, C. C. L., Fonslow, B., Delahunty, C., Gao, Y., Shah, H., and Yates, J. R. (2015) ProLuCID: An improved SEQUEST-like algorithm with enhanced sensitivity and specificity. *J. Proteomics 129*, 16−24.
(19) Medina-Cleghorn, D., Bateman, L. A., Ford, B., Heslin, A., Fisher, K. J., Dalvie, E. D., and Nomura, D. K. (2015) Mapping Proteome-Wide Targets of Environmental Chemicals Using Reactivity-Based Chemoproteomic Platforms. *Chem. Biol. 22*, 1394−1405.
(20) Benjamin, D. I., Louie, S. M., Mulvihill, M. M., Kohnz, R. A., Li, D. S., Chan, L. G., Sorrentino, A., Bandyopadhyay, S., Cozzo, A., Ohiri, A., Goga, A., Ng, S.-W., and Nomura, D. K. (2014) Inositol phosphate recycling regulates glycolytic and lipid metabolism that drives cancer aggressiveness. *ACS Chem. Biol. 9*, 1340−1350.

DOI: 10.1021/acschembio.7b00020
ACS Chem. Biol. XXXX, XXX, XXX−XXX